Directional Fluorescence Spectral Narrowing in All-Polymer Microcavities Doped with CdSe/CdS Dot-in-Rod Nanocrystals

Giovanni Manfredi[†], Paola Lova[†], Francesco Di Stasio[††], Roman Krahne[††], Davide Comoretto[†]*

† Dipartimento di Chimica e Chimica Industriale, Università di Genova, Genova, Italy

†† Nanochemistry dept., Istituto Italiano di Tecnologia, Genova, Italy

---

SUPPORTING INFORMATION

Supporting Information, Figure S1a, shows a TEM micrograph of the DiRs recorded using a JEOL-1100 TEM with acceleration voltage of 100 kV. The average core size is 4.1 nm, while rods diameter is 4.7 ± 0.5 nm. Supporting Information, Figure S1b shows nanocrystals length distribution retrieved from the TEM image reported in Supporting Information, Figure S1a. The statistics of the nanorod size distribution shows a dominant population with a length centered around 35 nm. However, a significant portion of nanorods with much shorter length, ranging essentially from 5 to 25 nm, is also observed and is considered as impurities.

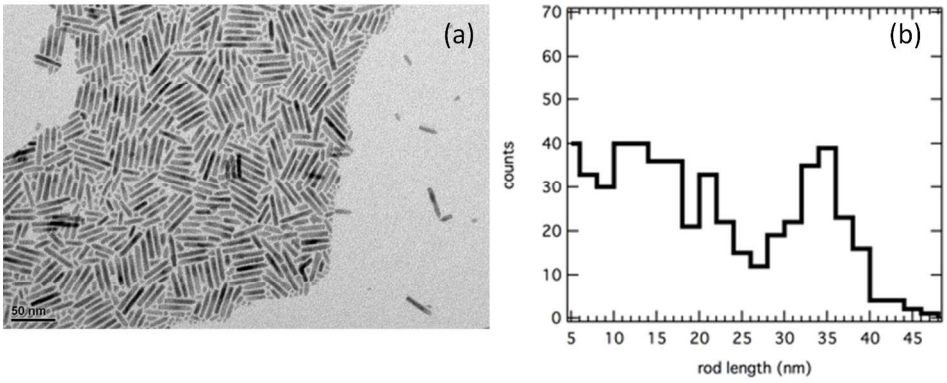

Figure S1: (a) TEM micrograph of CdSe/CdS DiRs. (b) Size distribution of DiRs retrieved from TEM data.

Supporting Information, Figure S2 shows confocal reflection (a) and fluorescence microscopy (b) images of the DiRs:PS nanocomposite film. A clear and homogeneous distribution of sub-micron scale DiRs is observed. Notice that size resolution of these techniques cannot be compared with TEM micrographs. In spite of the difference in the absorption spectrum with respect to the suspension, the PL emission is not modified (Figure 2a and b, main text). This testifies that no DiRs coalescence or sintering occurs in the highly-concentrated nanocomposite.

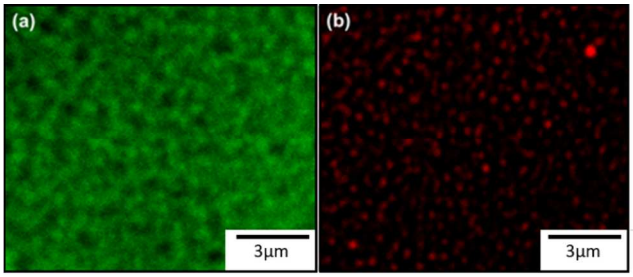

Figure S2: Optical confocal microscopy images of the DiRs:PS nanocomposite film. (a) Reflection of a laser at 514 nm wavelength integrated over 500-550 nm. (b) DiRs fluorescence excited with a laser at 405 nm and recorded in the 575-625 integrated spectral range in the same spot as in (a).

PL spectra of the reference can be de-convolved into two Voigt-like (convolution of Gaussian and Lorentz, as reported in Supporting Information, Equation S1) functions separated by about 10 nm.

$$y = y_0 + A \cdot \frac{2\ln 2}{\pi^{\frac{3}{2}}} \frac{w_L}{w_G^2} \cdot \int_{-\infty}^{+\infty} \frac{e^{-t^2}}{\left(\sqrt{\ln 2}\frac{w_L}{w_G}\right)^2 + \left(\sqrt{4\ln 2}\frac{x - x_c}{w_G} - t\right)^2} dt \qquad \text{(S1)}$$

In **Supporting Information, Equation S1,** y_0 is a baseline value, A is the area (in nm) of the Voigt function, w_L is the width of the lorentzian function and w_G is the width of the Gaussian function. The presence of two emissions is correlated to the bimodal DiRs size distribution shown in Supporting Information, Figure S2b.

The result of the deconvolution is shown in **Supporting Information, Figure S3a**. There, the two dashed lines positioned at 610.5 and 615.5 nm indicates the spectral integration range of our time corre-

lated single photon counting (TCSPC) measurements (Figure 4 in the main text) used to investigate the microcavity decay. Supporting Information, Table S1 reports the fitting parameters. Integrating the two peaks within the indicated spectral range, the ratio of the two areas (number of emitted photons) is 0.54 which is in good agreement with the ratio of the weights of the two faster components in the measured PL decay (0.57). Supporting Information Figure S3b shows a ratio spectrum that is obtained by dividing the fit to peak2 by the fit to peak1 (where peak 1 and peak 2 constitute the two components of the PL). This shows that peak 1, i.e. the component assigned to impurities, has its main contribution around 600 nm, where the ratio spectrum shows its minimum. On the other hand, peak 2 (due to long DiRs) dominates at about 630 nm where the ratio spectrum is maximum.

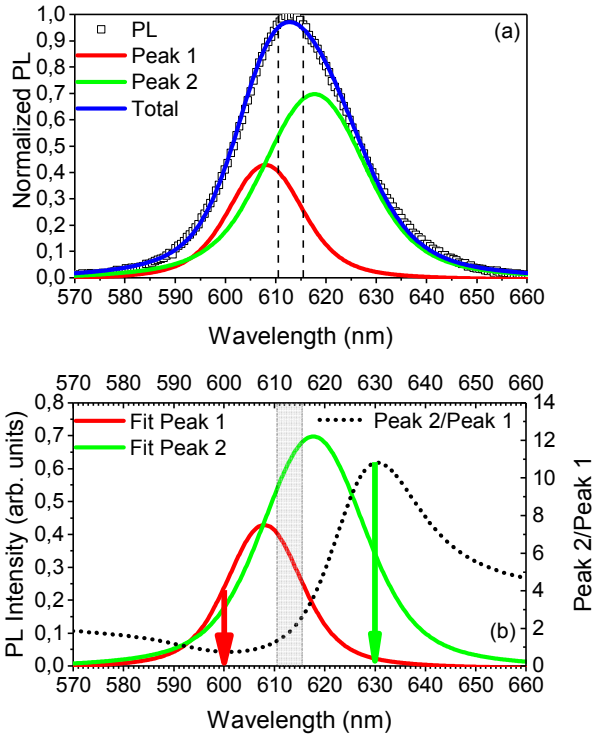

Figure S3: (a): Deconvolution of the PL spectrum of the DiRs:PS nanocomposite reference film (blue line), peak 1 component (red), peak 2 component (green); (b): comparison of the peak 1 and peak 2

components, showing their spectral ratio (peak2/peak1) as dotted line. Arrows show spectral position where time resolved PL is recorded: 600 nm, mainly peak 1; 630 nm, mainly peak 2.

Table S1: Parameters of the fitted functions.

	x_c (nm)	Area (nm)	W_G (nm)	W_L (nm)
Peak 1	608	10	13	8
Peak 2	617	22	18	11

To model the optical response of the microcavity, we used the PVK and CA refractive index dispersions previously reported.[1] However, the optical functions were unknown for the nanocomposite. To estimate its complex refractive index, we have first assumed that the DiRs have a small effect on the real part of the nanocomposite optical function, which is in turn very similar to that of PS.[2] A first tentative fit of the optical response of the microcavity has then been conducted neglecting DiRs absorption and obtaining a first estimation of the system layers thicknesses. However, having NCs absorption a clear effect on the microcavity, we deduced an extinction coefficient for the nanocomposite exploiting the thickness previously obtained from the microcavity fit and combining it to the absorbance spectra of a reference film. The procedure used was the following:

-The reference film is composed by a glass substrate, a CA layer and the nanocomposite layer as discussed in the main text. Being spin coating sensitive to the substrate material, the CA layer is added to obtain the same growing conditions of the DiRs:PS layer in microcavity.

-The absorbance spectrum of the reference and of the glass substrate are recorded.

-The reference absorbance (A_c) is corrected subtracting the out-of-resonance effect of reflection losses.

-The extinction coefficient k is calculated as $A_c = log\frac{1}{T} = 0.43\alpha d = 0.43\frac{4\pi k}{\lambda}d$ where λ is the wavelength and d is the thickness of the nanocomposite layer as obtained by the overall microcavity response fit.

-For λ>700 nm we considered the extinction coefficient negligible.

-The procedure is repeated until the new thickness is identical to the previous one within 5%.

-The DiRs:PS nanocomposite complex refractive index n_{PS}+ik is then used to fit the new layer thickness.

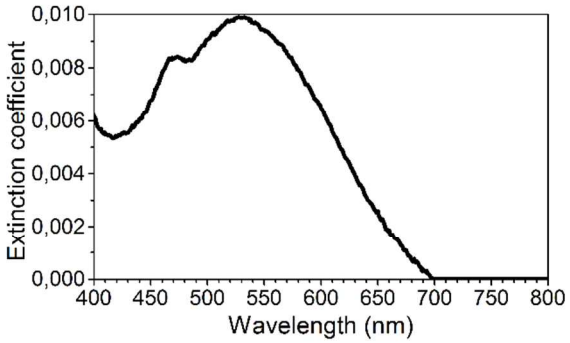

Figure S4: Extinction coefficient of the DiRs:PS nanocomposite**.**

Supporting Information, Figure S5a shows the transmittance spectra (as contour plots) of the microcavity recorded for different angles of incidence for S- and P-polarization (upper and lower part of the panel, respectively). In Supporting Information, Figure S5b the calculated spectra are reported for comparison. The intensity is given by a color code, while the incidence angle varies on the vertical axis and the wavelength is reported in the horizontal axis. The transmittance intensity is color coded going from blue (low transmittance) to red (high transmittance) as shown in the scale on the right side of the plot. The blue band is the signature of the PBG and its angle dependence is in full agreement with calcu-

lations confirming once more the optical quality of our microcavities. The fringes outside of the band gap are visible as yellow-greenish/red bands. The cavity mode, even if is not strongly pronounced, is visible as a tiny grey line inside the blue PBG band. Its weakness is justified by the overlap with the absorption tail of the DiRs:PS nanocomposite as discussed in the main text (Figure 2b).

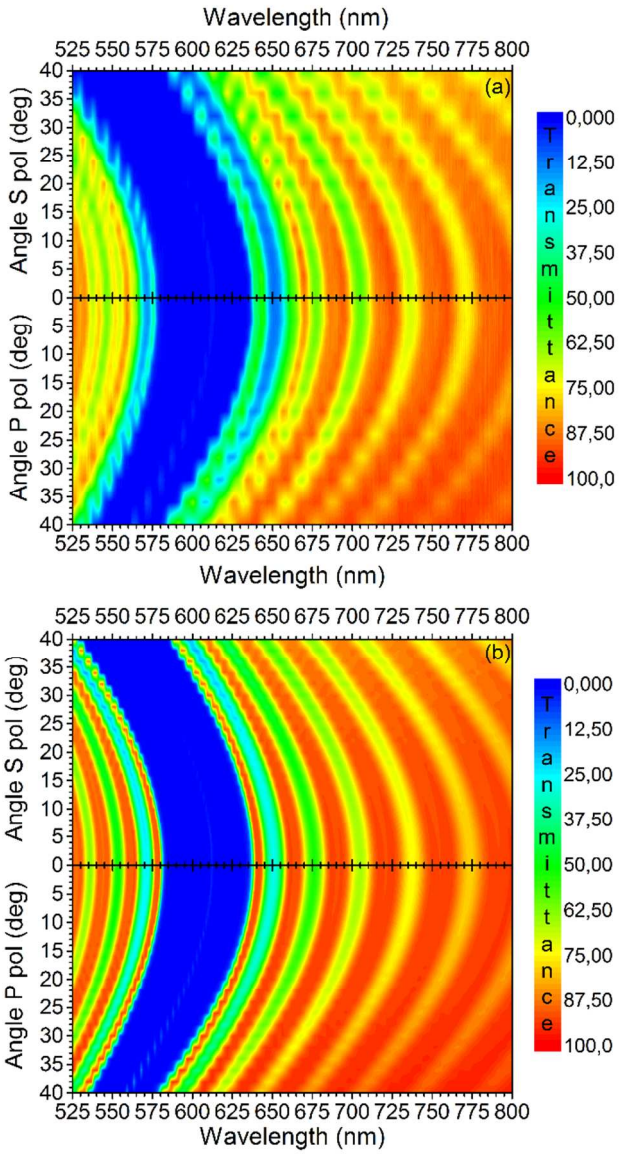

Figure S5: (a) Experimental and (b) calculated transmittance spectra of the microcavity as a function of the incidence angle for S- (upper panel) and P-polarized (lower panel) light.

To better appreciate the narrowing effect caused by the microcavity on the nanocrystals fluorescence spectrum, **Supporting Information, Figure S6** shows the peak normalized PL spectra of the microcavity and of the reference film. The ten-times reduction of the FWHM is clearly observed.

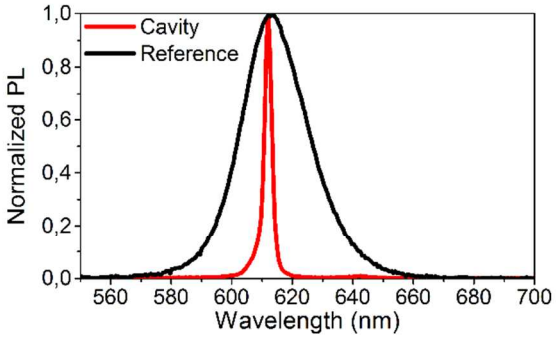

Figure S6: Peak normalized PL spectra for the microcavity (red line) and the reference DiRs:PS nanocomposite film (black line).

Supporting Information, Figure S7 shows PL spectra measured for different detection angles. The PL peak blue-shifts increasing the collection angle. Moreover, the intensity decreases due to the worsening of the spectral overlap between the cavity mode and the DiRs nanocomposite PL spectrum, which reduces the PL intensity enhancement effect. The angular dispersion of the PL spectra is in full agreement with the transmittance spectra unambiguously demonstrating that the PL sharpening is due to the cavity mode.

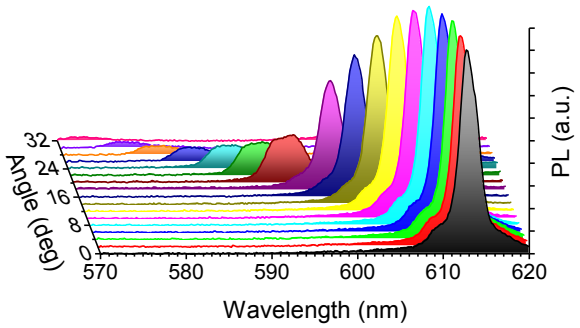

Figure S7: Microcavity PL spectra as a function of the detection angle.

Supporting Information, Figure S8 shows the PL decay of DiRs in toluene suspension. Even in this case, a tri-exponential decay allows to fit the data (see Supporting Information, Table S2 for fitting parameters).

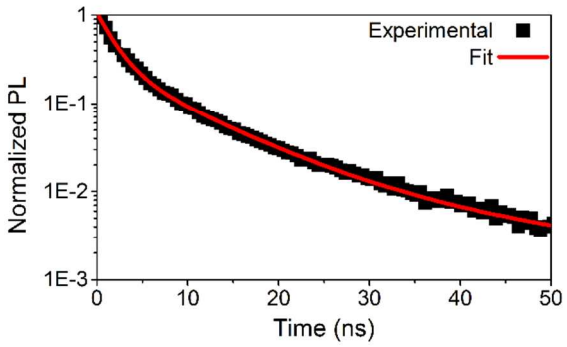

Figure S8: Spectrally integrated PL decay for NCs in toluene suspension.

Table S2: Lifetime (τ_j) and relative intensity (A_j) of the different PL decays for DiRs in toluene suspensions.

	τ_1 (ns)	A_1	τ_2 (ns)	A_2	τ_3 (ns)	A_3	PL QY (%)
Toluene suspension	2.0	0.77	9.5	0.22	39.0	0.01	>60

References

(1) Fornasari, L.; Floris, F.; Patrini, M.; Comoretto, D.; Marabelli, F., Demonstration of fluorescence enhancement via Bloch surface waves in all-polymer multilayer structures. Phys. Chem. Chem. Phys. 2016, 18, 14086-14093.

(2) Frezza, L.; Patrini, M.; Liscidini, M.; Comoretto, D., Directional Enhancement of Spontaneous Emission in Polymer Flexible Microcavities. J. Phys. Chem. C 2011, 115, 19939-19946.

(3) Angeloni, I.; Raja, W.; Brescia, R.; Polovitsyn, A.; De Donato, F.; Canepa, M.; Bertoni, G.; Proietti Zaccaria, R.; Moreels, I., Disentangling the Role of Shape, Ligands, and Dielectric Constants in the Absorption Properties of Colloidal CdSe/CdS Nanocrystals. ACS Photonics 2016, 3, 58-67.